Applied Mathematics and Nonlinear Sciences
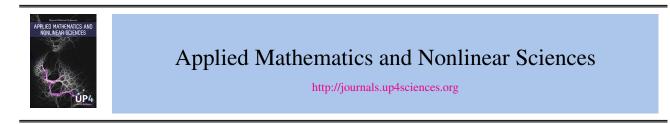
A Comparison between Integer and Fractional Order PD$^\mu$ Controllers for Vibration Suppression

Isabela R. BIRS[a][†], Cristina I. MURESAN[a], Silviu FOLEA[a], and Ovidiu PRODAN[b].

[a]Technical University of Cluj-Napoca, Department of Automation
ROMANIA

[b]Technical University of Cluj-Napoca, Department of Structural Mechanics
ROMANIA

Abstract

Along the years, unwanted vibrations in airplane wings have led to passenger discomfort. In this study, the airplane wing is modeled as a cantilever beam on which active vibration suppression is tested. The paper details the tuning of both integer and fractional order Proportional Derivative type controllers based on constraints imposed in the frequency domain. The controllers are experimentally validated and the results prove once more the superiority of the fractional order control approach.

1 Introduction

By suppressing unwanted vibrations in real life applications, significant improvements can be made in increasing safety and reducing discomfort for the passengers of an airplane, spectators on a stadium or construction workers on a bridge. Vibrations can be mitigated passively by means of tuned mass dampers that increase the mass and stiffness of flexible structures [1], or actively by means of sensors and actuators.

Many active control algorithms have been developed and the efficiency of the closed loop system depends on the chosen algorithm. Direct proportional feedback [2], constant gain velocity feedback control [3], optimal

---

[†]Corresponding author.
Email address: isabela.birs@aut.utcluj.ro

control strategies [4, 5], fuzzy logic controllers [6–8], robust control [9], and neural networks [10] are just a few of the approaches embraced to mitigate vibrations.

In the case of smart beam vibration suppression, fractional order PID controllers were proposed [11, 12] with good results, as well as fractional order PD controllers [13–15]. In the case of the fractional PID, its complexity represents a great disadvantage since there are five parameters that need to be tuned leading to solving a system of minimum five equations [16]. Alternative tuning methods are presented in [12] and [13] based on lowering the resonant peak on the frequency domain magnitude plot using optimization algorithms. The method proves useful in bringing a dramatic improvement in terms of settling time, but it does not tackle the robustness of the closed loop system.

In this study, two Proportional Derivative controllers were tuned using the same tuning method, making them eligible for an accurate comparison. Both controllers were tuned based on frequency domain specifications such as the gain crossover frequency, phase margin and robustness to gain variations. For the gain crossover frequency and the phase margin certain values are imposed, while the robustness is ensured by forcing the phase of the open loop system to be a straight line near the crossover frequency [17]. This type of tuning procedure has been discussed before, with numerous applications [16, 18–22]. However, its application to the problem of active smart beam vibration control is an original element of this manuscript.

The obtained controllers were tested on an experimental vibration stand built at the Technical University of Cluj-Napoca, Romania. The impulse responses of the closed-loop of the system were compared in terms of settling time and robustness.

The article is structured as follows: in the second section the tuning equations are detailed, in the third section the practical stand and the experimental results are presented, while the fourth section consists of conclusions.

2 Fractional and integer order controller tuning

In the study, two PD controllers were tuned with the purpose of suppressing unwanted vibrations. The parameters of both controllers were computed based on constraints imposed in the frequency domain: gain crossover frequency ω_{cg}, phase margin φ_m, and robustness. The constraints imposed indirectly ensure the settling time and the damping of the closed loop system in the time domain.

Knowing that the value of the magnitude at the gain crossover frequency is 1 (0 dB), the gain crossover specification can be mathematically written as

$$\left| \left(H_{\text{open-loop}}(j\omega_{cg}) \right) \right| = 1. \tag{1}$$

The equation for the phase margin constraint is expressed using the phase equation for the open loop system as:

$$\angle \left(H_{\text{open-loop}}(j\omega_{cg}) \right) = -\pi + \varphi_m.$$

The last specification imposed in the calculus of the controllers is the robustness. This condition guarantees an almost constant overshoot when the gain varies. One way to ensure this requirement is by imposing a constant phase in the interval grasping the gain crossover frequency. A constant phase is characterized by a straight line on the phase plot. This means that the derivative of the phase will be 0 when ω is equal to ω_{cg}. Mathematically expressing the robustness condition gives

$$\left. \frac{d \left(\angle H_{\text{open-loop}}(\omega) \right)}{d\omega} \right|_{\omega = \omega_{cg}} = 0. \tag{2}$$

For a process described by the transfer function noted $G(s)$, joined by a controller $C(s)$, the open loop equation is

$$H_{\text{open-loop}}(s) = G(s) \cdot C(s). \tag{3}$$

Rewriting the frequency domain specifications (1)-(2) in the complex plane with respect to (3), the constraints can be re-written as

$$\angle C(j\omega_{cg}) = -\pi + \varphi_m - \angle G(j\omega_{cg})$$

$$|C(j\omega_{cg})| = \frac{1}{|G(j\omega_{cg})|}$$

$$\left.\frac{\mathrm{d}(C(j\omega))}{\mathrm{d}\omega}\right|_{\omega=\omega_{cg}} + \left.\frac{\mathrm{d}(\angle G(j\omega))}{\mathrm{d}\omega}\right|_{\omega=\omega_{cg}} = 0. \tag{4}$$

The tuning of the controllers is made by replacing $C(j\omega)$ with the fractional and integer order PD transfer functions.

2.1   Fractional order PD controller tuning

The fractional order PD controller transfer function is

$$\mathrm{H_{FO\text{-}PD}}(s) = k_p\left(1 + k_d\, s^\mu\right), \tag{5}$$

where μ is the fractional order of the differentiator belonging to the interval $(0,2]$, k_p is the proportional gain, k_d is the derivative gain, and s is the Laplace variable. If $\mu = 1$ or $\mu = 2$, the controller is an integer order PD controller.

Replacing s with $j\omega$, we obtain the complex form of the fractional order controller:

$$\mathrm{H_{FO\text{-}PD}}(j\omega) = k_p\left[1 + k_d\,\omega^\mu\left(\cos\left(\frac{\pi\mu}{2}\right) + j\sin\left(\frac{\pi\mu}{2}\right)\right)\right]. \tag{6}$$

Replacing Eq. (6) in (4) gives

$$\left|k_p\left[1 + k_d\,\omega_{cg}^\mu\left(\cos\left(\frac{\pi\mu}{2}\right) + j\sin\left(\frac{\pi\mu}{2}\right)\right)\right]\right| = \frac{1}{|G(j\omega_{cg})|}$$

$$\angle\left[1 + k_d\,\omega_{cg}^\mu\left(\cos\left(\frac{\pi\mu}{2}\right) + j\sin\left(\frac{\pi\mu}{2}\right)\right)\right] = -\pi + \varphi_m - \angle G(j\omega_{cg})$$

$$\left.\frac{\mathrm{d}\left(\angle\left[1 + k_d\,\omega^\mu\left(\cos\left(\frac{\pi\mu}{2}\right) + j\sin\left(\frac{\pi\mu}{2}\right)\right)\right]\right)}{\mathrm{d}\omega}\right|_{\omega=\omega_{cg}} = -\left.\frac{\mathrm{d}(\angle G(j\omega))}{\mathrm{d}\omega}\right|_{\omega=\omega_{cg}}. \tag{7}$$

Focusing on the phase equation from Eq. (4) and expanding it further leads to

$$\frac{k_d\,\omega_{cg}^\mu\sin\left(\frac{\pi\mu}{2}\right)}{1 + k_d\,\omega_{cg}^\mu\cos\left(\frac{\pi\mu}{2}\right)} = \tan(-\pi + \varphi_m - \angle G(j\omega_{cg})), \tag{8}$$

while expanding the robustness condition leads to

$$\frac{\mu\,k_d\,\omega_{cg}^{\mu-1}\sin\left(\frac{\pi\mu}{2}\right)}{1 + 2k_d\,\omega_{cg}^\mu\cos\left(\frac{\pi\mu}{2}\right) + k_d^2\,\omega_{cg}^{2\mu}} = -\left.\frac{\mathrm{d}(\angle G(j\omega))}{\mathrm{d}\omega}\right|_{\omega=\omega_{cg}}. \tag{9}$$

Determining the controller parameters k_p, k_d and μ is done by solving the equations. The two parameters k_d and μ can be determined by solving the system of equations composed by Eqs. (8) and (9). An easy approach to system solving is the graphic method which consists of plotting k_d as functions of μ, based on Eqs. (8) and (9), and knowing that the solution is found at the intersection of these two plots.

After the derivative gain k_d and the fractional order of the differentiator μ are determined, k_p is easily computed using the following equation, derived from the magnitude condition in Eq. (7):

$$k_p = \frac{1}{|G(j\omega_{cg})|} \frac{1}{\sqrt{1 + 2k_d\,\omega_{cg}^{\mu} \cos\left(\frac{\pi\mu}{2}\right) + k_d^2\,\omega_{cg}^{2\mu}}}.$$

2.2   Integer order PD controller tuning

The tuning of the integer order PD controller is done similarly to the fractional order one starting from its transfer function:

$$\mathrm{H_{PD}}(s) = k_p\,\frac{T_d\,s + 1}{T_N\,s + 1}, \tag{10}$$

where T_d is the derivative time constant and T_N is the filter time constant. For a derivative effect, it is imposed that T_N is much smaller than T_d. The integer order PD controller in Eq. (10) has exactly the same tuning parameters as the fractional order controller in Eq. (5). Thus, the same performance specifications at Eqs. (1)-(2) are used to tune the integer order PD controller. Using the phase condition in (4), it follows that:

$$\angle\left(k_p\,\frac{T_d\,j\omega_{cg} + 1}{T_N\,j\omega_{cg} + 1}\right) = -\pi + \varphi_m - \angle G(j\omega_{cg}). \tag{11}$$

Denoting the right-hand side of Eq. (11) as $z = \tan(-\pi + \varphi_m - \angle G(j\omega_{cg}))$, the last equation can be expressed as:

$$T_D(\omega_{cg} - zT_N\omega_{cg}^2) - T_N\omega_{cg} + z = 0. \tag{12}$$

The robustness condition in Eq. (4) leads to

$$\frac{T_d}{1 + T_d^2\omega_{cg}^2} - \frac{T_N}{1 + T_N^2\omega_{cg}^2} = -\left.\frac{\angle G(j\omega_{cg})}{\mathrm{d}\omega}\right|_{\omega=\omega_{cg}}. \tag{13}$$

Denoting $-\left.\dfrac{\angle G(j\omega_{cg})}{\mathrm{d}\omega}\right|_{\omega=\omega_{cg}} = x$, the last equation in Eq. (13) leads to

$$T_d^2 T_N\omega_{cg}^2 - T_d(1 + T_N^2\omega_{cg}^2) + T_N + x = 0. \tag{14}$$

Then, based on Eq. (12) and (14), the derivative and filter time constants can be easily computed. Once these have been determined, using the magnitude condition in (4), the following result is obtained:

$$\left|k_p\,\frac{T_d\,j\omega_{cg} + 1}{T_N\,j\omega_{cg} + 1}\right| = \frac{1}{|G(j\omega_{cg})|},$$

which can be used to determine the proportional gain k_p:

$$k_p = \frac{\sqrt{T_N^2\omega_{cg}^2 + 1}}{|G(j\omega_{cg})| \cdot \sqrt{T_d^2\omega_{cg}^2 + 1}}.$$
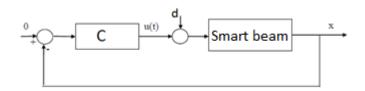
Fig. 1 Active vibration attenuation in a smart beam.

3 Active vibration suppression in a smart beam

Since both controllers were tuned with similar methods based on imposed frequency domain specifications, in order to properly analyze and compare their real life behavior, both were tested on the same equipment under the same conditions.

The schematic of the closed loop system is depicted in Fig. 1. Since the main purpose of the controller is to cancel the oscillations of the beam, the reference position will always be kept at 0. The measured structural displacement is given to the controller, which computes the control signal $u(t)$ which is the control force for the actuator. The controller will treat any excitation as a disturbance, continuously trying to reject it. In the subsequent paragraphs, the disturbance d in Fig. 1 will be considered as an impulse disturbance.

3.1 Description of the practical stand and model identification

The experimental setup has been entirely developed at the Technical University of Cluj-Napoca, Romania. The most important part of the stand is the smart beam which is 240 mm long, 40 mm broad, and 3 mm narrow. The beam is fixed on one end, while the other is allowed to vibrate freely. The beam is "smart" because its location is permanently known with the help of two Honeywell SS495A Miniature Ratiometric Linear (MRL) Hall Effect sensor. The experimental setup can be seen in Fig. 2.

Fig. 2 Active vibration attenuation in a smart beam.

On the surface of the beam there are two magnets that were hot pressed into its surface. The position of the smart beam is controlled by controlling the current/voltage through the coils which controls the magnetic flux, attracting the magnets, hence the beam. The coils can only attract the beam without offering the possibility to reject it. Only Coil 1 is used for vibration attenuation, while Coil 2 is used to give measurable impulse type disturbances. The reason that Coil 1 is used for control is the fact that it is closer to the fixed end of the beam, making it easier to stop the beam's movements.

The National Instruments modules NI 9215 and NI 9263 are used to read data from the sensors and to control the magnetic flux in the coils. The control algorithm was implemented using LabVIEWTM and the real time CompactRIO$^{\mathrm{TM}}$ 9014 controller. The sample rate is 1 ms.

The model was experimentally identified as a second order transfer function based on data acquired by giving an impulse on Coil 1. A swept sine having frequencies in the range $[5, 60]$ Hz has been applied to the

beam. Based on the measured data, the resonant frequency of the beam has been determined to be at 15 Hz. Transforming 15 Hz to rad/s, the natural frequency ω_n was determined to be 95 rad/s. The second order model obtained is:

$$G(s) = \frac{1.245}{s^2 + 1.14s + 9025}. \tag{15}$$

The overlay of the impulse response of $G(s)$ and the experimental data is shown in Fig. 3. For comparison purposes, 6th and 10th order models were also identified improving the fit, but also increasing the controller calculus. Thus, the second order approximation given in Eq. (15) is used for controller tuning.
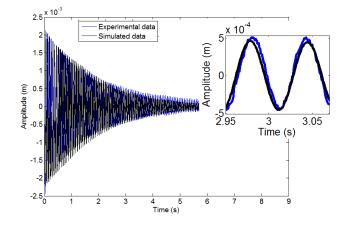

Fig. 3 Experimental and simulation of impulse response of the smart beam.

3.2   Experimental results

The Bode diagram of the uncompensated structure is illustrated in Fig. 4. Both controllers were designed based on frequency domain constraints. The imposed gain crossover frequency was $\omega_{cg} = 250$ rad/s and the phase margin $\varphi_m = 65$, as well as the robustness condition. These frequency domain specifications have been used in order to compute the parameters of both integer and fractional order controllers. Note that the same specifications are used in tuning.

The controllers that were computed using the method explained in the previous section are:

$$\begin{aligned} \text{H}_{\text{FO-PD}}(s) &= 465.9 \cdot \left(1 + 1.65\, s^{0.728}\right) \\ \text{H}_{\text{PD}}(s) &= 9727.8 \cdot \frac{0.0177s + 1}{8.7029 \cdot 10^{-4}\, s + 1}. \end{aligned} \tag{16}$$

Remark. Analyzing the structure of the tuned controllers, it can be observed that the integer order proportional-derivate controller is implemented using a low pass filter, while the fractional order is implemented using the ideal structure. The low pass filter ensures a proper transfer function representation of the integer order PD controller, as well as an equal number of tuning parameters in comparison to the fractional order PD controller, such that the same tuning procedure is applied. In this case, both controllers are expected to achieve similar closed loop performance results.

The frequency domain response of the open loop with both controllers is plotted in Fig. 5. As can be seen, both the gain crossover and the phase margin specifications are honored. The main difference between the controllers is the robustness specification. When the tuning was performed, the phase line including the phase margin was imposed to be a flat line. The fractional order controller makes the phase flat on a longer interval than the integer order one, leading, in this particular situation, to a more robust system to gain variations. This
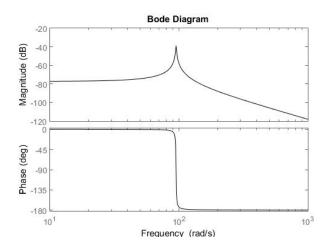
Fig. 4 Bode diagram of the uncompensated structure.

will be further analyzed in the impulse response of the closed loop system and by performing a simple practical robustness test.
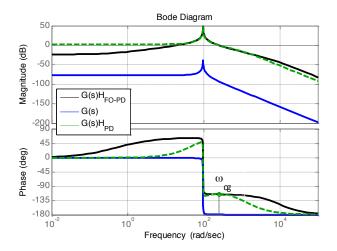

Fig. 5 Frequency response of the uncompensated smart beam and of the open loop systems with fractional and integer order PD controllers.

In order to implement the controllers on the practical vibration unit, the digital forms of the two controller transfer functions in Eq. (16) have to be obtained first. Since the sensors read the position of the beam every 1 ms, the sampling time of the discretization has to be kept the same, $T_s = 0.001$ s. The problems arise in implementing the fractional order transfer function. A novel digital implementation used to approximate fractional order transfer functions to integer order ones [23] consists in generating a function that maps the Laplace operator s to the discrete time operator z^{-1}, followed by the evaluation of the frequency response of the discrete time system. The impulse response of the discrete time fractional order system is computed based on its frequency response. The final step consists in finding a rational discrete time transfer function having the same impulse response as the original discrete time fractional order system.

The practical results with the fractional order controller can be seen in Fig. 6. In the left plot, the impulse response of the uncompensated structure is presented. As it can be seen, the settling time is greater than 6 seconds. In the center plot, the impulse response of the closed loop system with the H$_{FO-PD}$ controller for two

consecutive tests is plotted, while in the right plot a zoomed impulse response is shown for a more detailed analysis. The closed loop settling time is less than 200 ms.
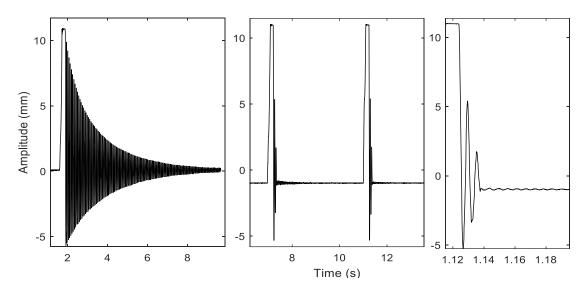

Fig. 6 Closed loop impulse response with the fractional order controller: free impulse response (left), active suppression (center), and zoomed active suppression (right).

The results obtained with the integer order controller can be seen in Fig. 7. The center and the zoomed impulse response plots (right) illustrate a greater settling time than in the case of the fractional controller. The number of oscillations until the vibration is completely cancelled is also greater. Comparing the zoomed impulse responses for both controllers, it is clear that the fractional order controller is superior to the integer order one.
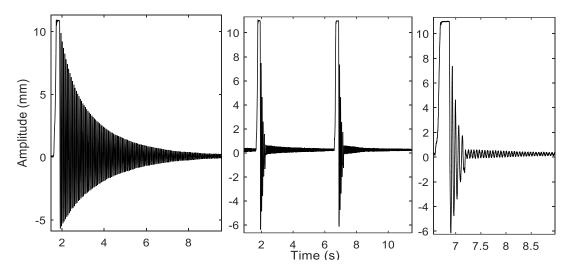

Fig. 7 Closed loop impulse response with the integer order controller: free impulse response (left), active suppression (center), and zoomed active suppression (right).

In order to practically compare the robustness of the two controllers a simple test was performed. Near the free end of the beam, a weight of 2 grams was attached bending and changing the initial position of the beam and indirectly the gain of the identified second order transfer function. The beam was then subjected to the same impulse excitation and the results can be seen in Fig. 8. Once more, the fractional order controller has an
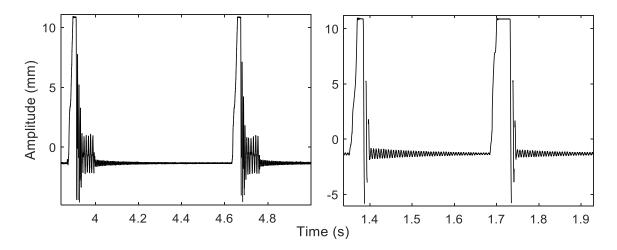
outstanding performance.

Fig. 8 Robustness tests performed on the closed loop system with integer (left) and fractional (right) controllers.

4 Conclusions

In this study, a fractional order and an integer order controller were tuned for vibration attenuation in a smart beam using the same method and the same frequency domain constraints: gain crossover frequency, phase margin and robustness. The robustness specification was imposed indirectly by imposing a flat phase around the crossover frequency. The experimental results, obtained by applying an impulse disturbance to the free end of the smart beam, demonstrate that the fractional order controller is more robust than the integer order one. Also, the fractional order controller mitigates vibrations in less time, making it the better choice to solve vibration attenuation problems.

References

[1] V. R. Tatavolu and S. R. Panchumarthy, (2013), Embedded computer based active vibration control system for vibration reduction of flexible structures, Journal of Computer Science, vol. 9, no. 7, pp. 838-846. doi 10.3844/jc-ssp.2013.838.846

[2] R.K. Kumar and S. Narayanan, (2008), Active vibration control of beams with optimal placement of sensor/actuator pairs, Smart Materials and Structures, vol. 17, 055008. doi 10.1088/0964-1726/17/5/055008

[3] S. Kaipura and M.Y. Yasin, (2010), Active vibration suppression of multilayered plates integrated with piezoelectric fiber reinforced composites using an efficient finite element model, Journal of Sound and Vibration, vol. 329, pp. 3247-3265. doi 10.1016/j.jsv.2010.02.019

[4] T. Roy and D. Chakraborty, (2009), Optimal vibration control of smart fiber reinforced composite shell structures using improved genetic algorithm, Journal of Sound and Vibration, vol. 319, pp. 15-40. doi 10.1016/j.jsv.2008.05.037

[5] H. Djojodihardjo, M. Jafari, S. Wiriadidjaja, and K. A. Ahmad, (2015), Active vibration suppression of an elastic piezoelectric sensor and actuator fitted cantilevered beam configurations as a generic smart composite structure, Composite Structures, vol. 132, pp. 848-863. doi 10.1016/j.compstruct.2015.06.054

[6] N. D. Zorić, A. M. Simonović, Z. S. Mitrović, S. N. Stupar, A. M.Obradović, and N. S. Lukić, (2014), Free vibration control of smart composite beams using particle swarm optimized self-tuning fuzzy logic controller, Journal of Sound and Vibration, vol. 333, pp. 5244-5268. doi 10.1016/j.jsv.2014.06.001

[7] M. Marinaki, M. Marinakis, and G.E. Stavroulakis, (2010), Fuzzy control optimized by PSO for vibration suppression of beams, Control Engineering Practice, vol. 18, pp. 618-629. doi 10.1016/j.conengprac.2010.03.001

[8] J. Wei, Z. Qiu, J. Han, and T. Wang, (2010), Experimental comparison research on active vibration control for flexible

piezoelectric manipulator using fuzzy controller, Journal of Intelligent and Robotic Systems, vol. 59, pp. 31-56. doi 10.1007/s10846-009-9390-2

[9] Y.-R. Hu and A. Ng, (2005), Active robust vibration control of flexible structures, Journal of Sound and Vibration, vol. 288, pp. 43-56. doi 10.1016/j.jsv.2004.12.015

[10] O. Abdeljaber, O. Avci, and D. Inman, (2016), Active vibration control of flexible cantilever plates using piezoelectric materials and artificial neural networks, Journal of Sound and Vibration, vol. 363, pp. 33-53. doi 10.1016/j.jsv.2015.10.029

[11] C. Onat, M, Sahin, and Y. Yaman, (2012), Fractional controller design for suppressing smart beam vibrations, Aircraft Engineering and Aerospace Technology, vol. 84, no. 4, pp. 203-212. doi 10.1108/00022661211237728

[12] I. R. Birs, C. I. Muresan, S.Folea, and O. Prodan, (2016), Vibration supression with fractional-order $PI^\lambda D^\mu$ controller, submitted to the IEEE International Conference on Automation, Quality and Testing, Robotics AQTR, 19-21 May, Cluj-Napoca, Romania, under review.

[13] O. Prodan, I. Birs, S. Folea, and C. Muresan, (2015), Seismic Mitigation in Civil Structures Using a Fractional Order PD, in The 3rd International Conference on Control, Mechatronics and Automation, Barcelona, Spain.

[14] C. I. Muresan and O. Prodan, (2014), Vibration Suppression in Smart Structures using Fractional Order PD controllers, IEEE International Conference on Automation, Quality and Testing, Robotics AQTR, pp. 1-5, 22-24 May, Cluj-Napoca, Romania. doi 10.1109/AQTR.2014.6857907

[15] C. I. Muresan, O. Prodan, and S. Folea, (2014), Tuning Method of Fractional Order Controllers for Vibration Suppression in Smart Structures, Applied Mechanics and Materials Journal, vol. 598, pp. 534-538. doi 10.4028/www.scientific.net/AMM.598.534

[16] C. A. Monje, Y.Q. Chen, B.M. Vinagre, D. Xue, and V. Feliu, 2010, Fractional order Systems and Controls: Fundamentals and Applications, Springer-Verlag, London.

[17] Y. Luo and Y. Chen, (2011), Stabilizing and robust FOPI controller synthesis for first order plus time delay systems, In Proceedings of the IEEE Conference on Decision and Control, pp. 2040-2045.

[18] C. I. Muresan, S. Folea, G. Mois, and E. H. Dulf, (2013), Development and implementation of an FPGA based fractional order controller for a DC motor, Mechatronics, vol. 23, no. 7, pp. 798-804. doi 10.1016/j.mechatronics.2013.04.001

[19] B. M. Vinagre, I. Podlubny, L. Dorcak, and V. Feliu, (2000), On Fractional PID Controllers: A Frequency Domain Approach, Proceedings of IFAC Workshop on Digital Control: Past, Present and Future of PID Control, Terrasa, Spain, pp. 53-58.

[20] P. Lanusse, J. Sabatier, and A. Oustaloup, (2014), Extension of PID to fractional orders controllers: a frequency-domain tutorial presentation, IFAC Proceedings Volumes, 19th IFAC World Congress, vol. 47, no. 3, pp. 7436-7442. doi 10.3182/20140824-6-ZA-1003.01053

[21] H. S. Li, Y. Luo, and Y. Q. Chen, (2010), A Fractional Order Proportional and Derivative (FOPD) Motion Controller: Tuning Rule and Experiments, IEEE Transactions on Control Systems Technology, vol. 18, no. 2, pp. 516-520. doi 10.1109/TCST.2009.2019120

[22] S. S. Bhase, M. J. Lengare, and B. M. Patre, (2015), Tuning of robust FO[PI] plus fractional lead controller for integrating time-delay systems, International Journal of Automation and Control (IJAAC) Vol. 9, no. 3. doi 10.1504/IJAAC.2015.070959

[23] R. De Keyser, C. Muresan, and C. Ionescu, (2016), A low-order computationally efficient approximation of fractional order systems, submitted to Automatica, under review.